Spin-glass-like behavior in mechanically alloyed nanocrystalline Fe-Al-Cu

J. A. De Toro, M. A. López de la Torre,* and J. M. Riveiro
Departmento de Física Aplicada, Universidad de Castilla–La Mancha, Campus Universitario, 13071 Ciudad Real, Spain

R. Sáez Puche, A. Gómez-Herrero, and L. C. Otero-Díaz
Departamento de Química Inorgánica, Universidad Complutense de Madrid, 28040 Madrid, Spain
(Received 29 April 1999)

We report on the magnetic properties of mechanically alloyed $Al_{49}Fe_{30}Cu_{21}$. The system was observed by high-resolution electron microscopy to be composed of nanosized solid solution grains embedded in an amorphous matrix of roughly the same composition. The irreversibility between the field-cooled and zero-field-cooled magnetization curves together with some ac susceptibility features closely resemble those exhibited by spin glasses. However, the analysis of the nonlinear susceptibility allowed us to rule out the existence of a true thermodynamic phase transition, since it was apparent the absence of a divergent increase in the nonlinear coefficients on approaching the freezing temperature. Surface effects are considered a minor source for the observed phenomena, remaining the blocking of interacting superparamagnetic moments the main mechanism to account for them. We discuss these three different origins for spin-glass-like behavior in the context of mechanically alloyed materials. [S0163-1829(99)04041-2]

I. INTRODUCTION

In the last few years the magnetic nature of mechanically alloyed (MA) or milled products have been the subject of a number of works. Some of them claim to have encountered ''concentrated'' bulk spin glasses[1–4] on the basis of dc magnetization irreversibility and ac susceptibility ''cusplike'' behavior. Other authors attribute such magnetic features to superparamagnetism[5] or spin disorder in the nanocrystals' boundaries.[6] Actually, considerable attention has been dedicated along the last two decades to a choice of criteria for distinguishing systems with a true spin-glass transition from superparamagnetic systems with clusters having a probability to overcome an anisotropy energy barrier.[7–11] Through the application of most of these criteria in a typically controversial case, this paper attempts to shed some light on the actual origin of the spin-glass-like (SGL) behavior often observed in mechanically alloyed systems.

MA seems to have two structural effects leading to SGL magnetic features: the reduction of crystallite size and the introduction of atomic disorder. When the size of the magnetic grains enters into the nanometer scale the single-domain configuration becomes energetically favorable and, provided they are exchange decoupled (e.g., embedded in a certain poorly conducting nonmagnetic matrix), the particles' moments rotate coherently if the thermal energy exceeds the anisotropy barrier; this magnetic behavior is described as superparamagnetism. Under certain conditions—as the existence of dipole interaction between particles and/or a narrow particle volume distribution—the magnetic properties of such systems can resemble very much those of spin glasses. When the grains are in contact, only separated by highly disordered grain boundaries, the ratio of these regions to the total volume becomes significant, exhibiting some SGL effects and shifted hysteresis loops similar to those shown by oxide nanoparticles[12,13] and by spin-valve systems,[14] but by no means could they be associated to a thermodynamic transition. On the other hand, if the atomic disorder, either structural (amorphous milled products[1]) or site disorder of the magnetic elements,[3] extends to the bulk it can provide magnetic Ruderman-Kittel-Kasuya-Yosida (RKKY) competition leading to frustration and the subsequent possibility for the formation of a true spin-glass phase. Thereby, it must be remarked that at least three different possible origins can be found in the literature for the SGL behavior observed in mechanically alloyed samples and, consequently, care must be taken in elucidating the actual primary mechanisms for each case.

In particular, the analysis of the temperature dependence of the nonlinear susceptibility (χ_{nl}) was established two decades ago[15,16] as the fundamental test to check the existence of a thermodynamic transition, hence providing a clear criterion to distinguish real spin glasses from ''spin-glass-like'' materials.[7]

As can be noticed, the determination of the kind of nanostructure involved is crucial in this context. In this paper we carried out a thorough structural study and then performed all the relevant dc and ac magnetic measurements on a sample of mechanically alloyed Fe-Al-Cu. The sample did show SGL behavior and then a χ_{nl} analysis was accomplished in order to ascertain whether its origin is a phase transition occurring at a well defined critical temperature or rather a dynamic nonequilibrium process extended over a certain temperature range.

II. EXPERIMENT

Four different mixtures of high-purity elemental Al, Cu, and Fe powders were prepared with nominal compositions $Fe_{30}(Al_{1-x}Cu_x)_{70}$, for $x=0$, 0.1, 0.2, 0.3. They were sealed under an Ar atmosphere in hardened stainless steel pots (100-cm^3 volume) containing 10-mm $\varnothing$ balls of the same material in a ball to powder mass ratio of 12:1. The mixtures were milled for 180 h at 225 rpm. Further details on the milling conditions can be found elsewhere.[17] The decrystal-

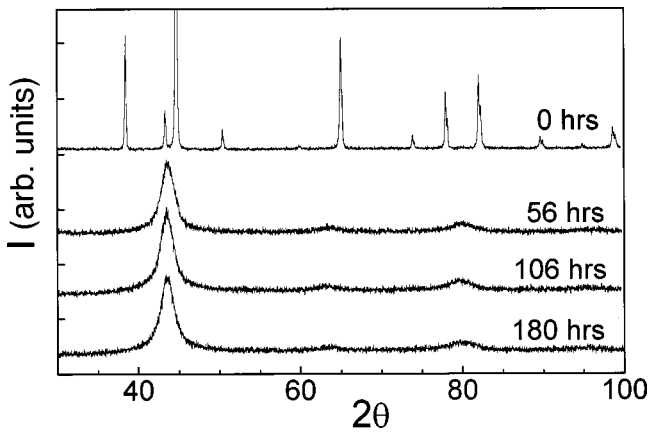

FIG. 1. Evolution of the AFC x-ray-diffraction spectra with milling time.

lizing process of the samples was monitored by x-ray diffraction (XRD) and, down to the micrometer stage, scanning electron microscopy (SEM). The present work will mainly be concerned with the properties of the product corresponding to $x=0.3$. The rest of the alloys presented more complex magnetic features, as will be explained below.

The structure of the sample was first studied by x-ray diffraction (XRD) using Cu $K\alpha$ radiation and 2θ geometry. Further insight was gained with a comprehensive transmission electron microscopy (TEM) study: conventional TEM in support of the high resolution work was done in a JEM 2000FX microscope operated at 200 kV, analytical data collection and selected area electron-diffraction (SAED) patterns were recorded in a CM200 FEG microscope operating in the nanoprobe mode (200 kV), and high-resolution electron microscopy (HRTEM) was carried out with a JEM 4000EX microscope operated at 400 kV. Acquisition and subsequent image processing of the HRTEM micrographs were accomplished with a charge-coupled device (CCD) camera and the GATAN Digital Micrograph software. The composition was checked by x-ray energy dispersive spectroscopy (XEDS).

dc magnetic measurements were carried out using a commercial superconducting quantum interference device (SQUID) magnetometer (Quantum Design) and a vibrating sample magnetometer (VSM) from LDJ Electronics. The same SQUID was employed in the ac susceptibility experiments.

III. RESULTS AND DISCUSSION

A. Structural characterization

The evolution of the sample x-ray-diffraction patterns with milling time (MT) is shown in Fig. 1. No changes were noticed after 180 h of milling. The rate of loss in saturation magnetization, mainly due to the progressive alloying of Fe, was also greatly attenuated after this point. Then, we will refer in the following, unless otherwise stated, to the $x=0.3$ sample milled for 180 h [$Al_{49}Fe_{30}Cu_{21}$(AFC)].

The last pattern in Fig. 1 corresponds, following the Halder-Wagner procedure,[18] to bcc grains of lattice parameter $a=2.95$ Å (0.08 Å larger than that of bcc Fe) and size—according to the Scherrer formula[19]—around 5 nm. Figure

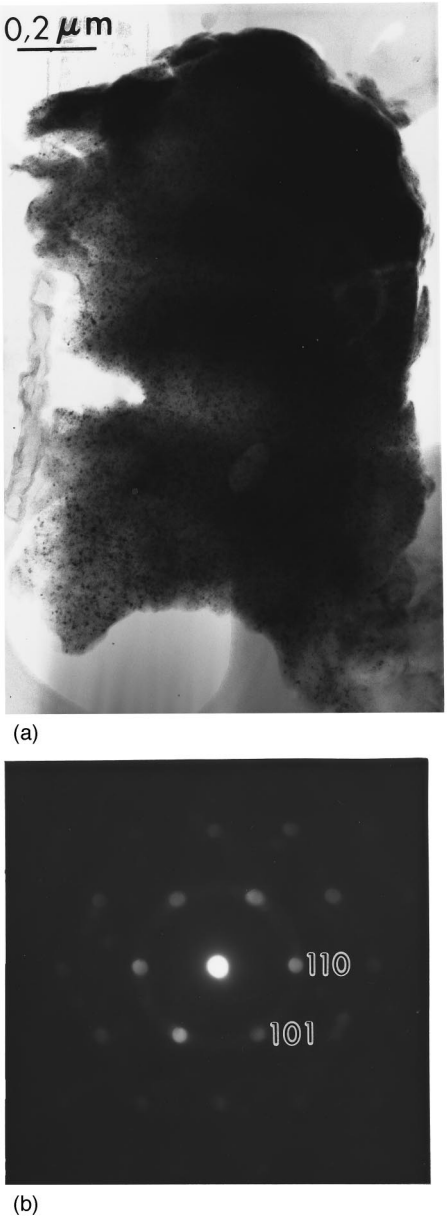

FIG. 2. (a) TEM micrograph showing nanocrystals (black spots) embedded in an amorphous matrix. (b) SAED pattern registered in one of the crystalline grains.

2(a) is a TEM micrograph showing an assembly of nanoparticles (black spots) embedded in a brighter matrix. The size of such particles agrees with the value estimated from the x-ray peaks. The electron-diffraction results further confirmed the particle crystallinity and structure as well as the amorphous character of the matrix. Figure 2(b) shows a SAED pattern registered in one of the black spots. It can be indexed as [111] zone axis of a bcc structure with lattice parameter $a=2.96$ Å, in close agreement with the value obtained from the x-ray pattern. Likewise, an amorphous halo is observed when selecting a region in the matrix. In the HRTEM image of Fig. 3(a) we can observe the lattice fringes of the crystalline grains in a disordered matrix. Figure 3(b) shows the corresponding Fourier transform (FT). Note the presence of a diffuse halo, typical of an amorphous material, and a ring of sharp reflections with a d spacing of 2.04 Å,

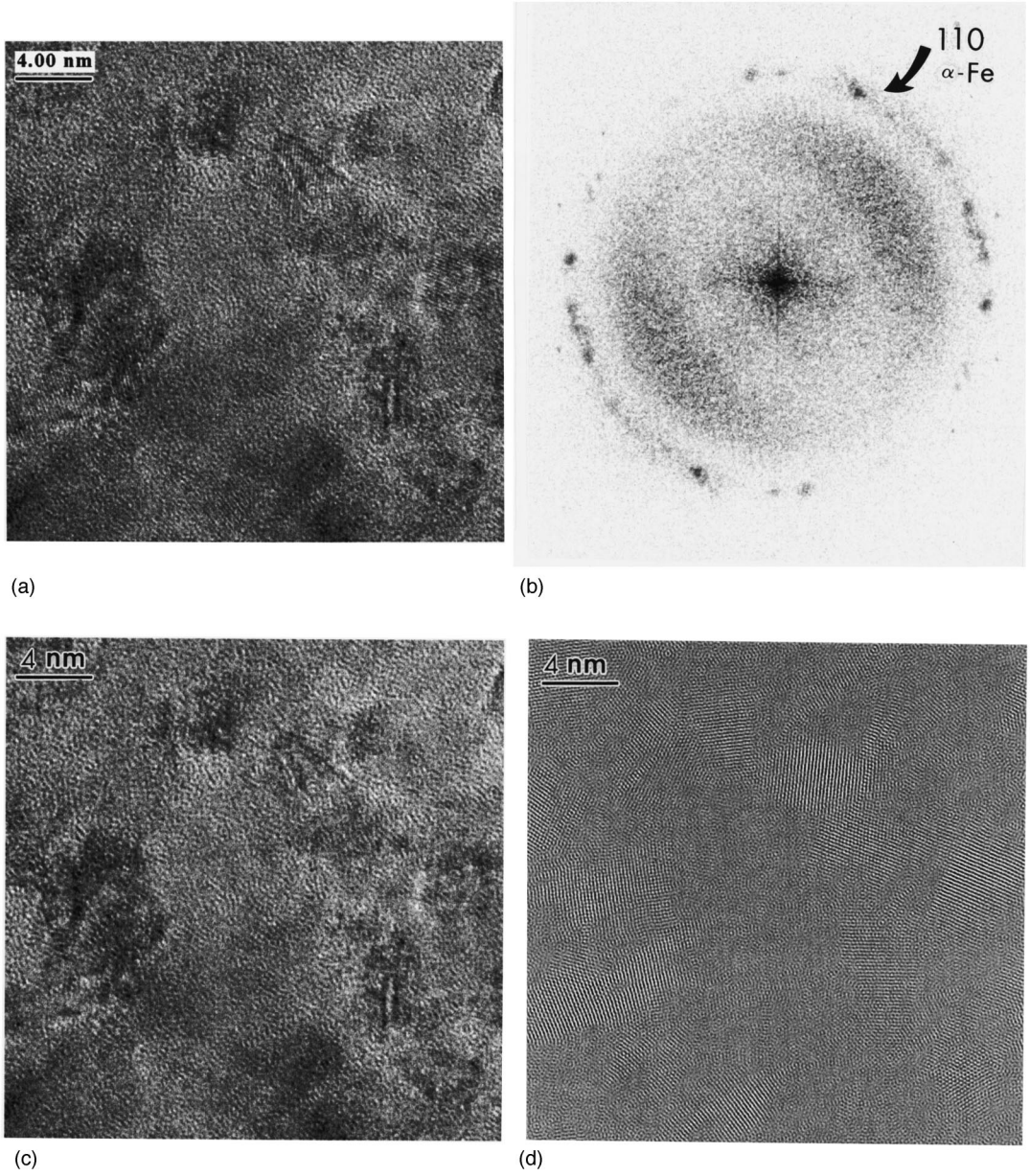

FIG. 3. (a) HRTEM micrograph showing crystalline fringes separated by highly disordered areas. (b) Corresponding SAED pattern. (c) Filtered image of the crystalline regions. (d) Filtered image of the amorphous region.

corresponding to the (110) planes of the bcc solid solution. The ring is not complete for the scattering took place only in a few grains. Figures 3(c) and 3(d) show two complementary Fourier filtered images of Fig. 3(a) constructed by applying the relevant annular filters in the pattern of Fig. 3(b) and subsequent inverse Fourier transform (IFT): the first one—obtained after filtering the outer ring—shows the typical homogeneous mottled contrast of amorphous materials, and the second one—after filtering the halo—exhibits clear fringes in the regions occupied by the nanocrystals.

The composition of the two phases, measured by x-ray energy dispersive spectroscopy (XEDS), turned out to be very similar: $Al_{38}Fe_{37}Cu_{21}O_4$ for the crystalline grains, and around 3% average less of Fe in the matrix. This indicates, comparing with the initial ratios before milling, slight oxidation and Fe enrichment (both around 4%). Although the commented structure was reached through a nonequilibrium technique, it is worth mentioning that the phase diagram of Fe-Al-Cu predicts the formation of a bcc solid solution for the observed composition.

B. Magnetic properties

In a previous work, we measured the field-cooled (FC) and zero-field-cooled (ZFC) magnetization curves of the four samples. For $x=0$ we observed two clear superimposed irreversibility phenomena (Fig. 2 in Ref. 17). The high-temperature one ($T_h \sim 120\,\mathrm{K}$) was characterized by a broad ZFC maximum, whereas the lower temperature ($T_1 \sim 25\,\mathrm{K}$) irreversibility was signaled by a relatively sharp ZFC peak. Both phenomena were reflected as well in ac susceptibility measurements. The measurement of the frequency sensitivity ($p = \Delta T_{\max} / \langle T_{\max} \rangle \Delta \log w$) of the high-temperature ac susceptibility maximum yielded a typical superparamagnetic

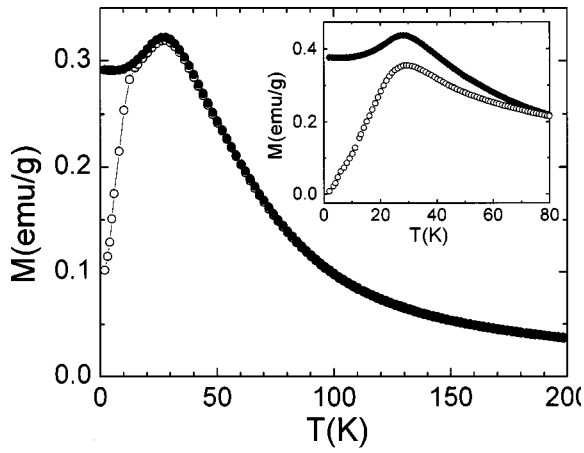

FIG. 4. FC and ZFC magnetization measured at 500 Oe. The inset shows the same curves measured at 50 Oe.

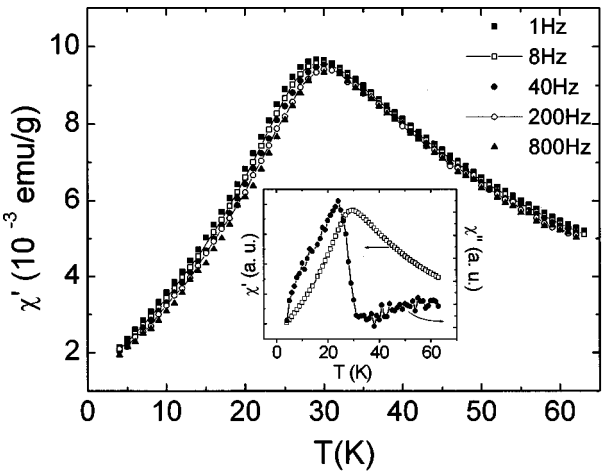

FIG. 5. Real component of the ac susceptibility vs temperature for different frequencies. The inset also shows the absorption component χ''—conveniently magnified for clarity—for the 8-Hz case. The solid lines are guides to the eye.

value[20] ($p \approx 0.1$), which confirmed that such maximum was due to the blocking of certain magnetic clusters. We observed that the high-temperature irreversibility diminished and the associated ZFC maximum smoothened as the Cu concentration increased, eventually disappearing for $x = 0.3$. Besides, after the publication of that work, a thorough XEDS analysis showed the minority presence of magnetite (Fe_3O_4) nanocrystals in all the samples. The amount of magnetite was estimated from numerous selected area analysis and subsequent statistics. The magnetite percentage was highest for $x = 0$ and was observed to progressively decrease with x along one order of magnitude. Therefore we conclude that the broad high-temperature ZFC maximum in the sample with $x = 0$ must be ascribed to the blocking of the magnetite nanoparticles and, consequently, these cannot be made responsible for the low-temperature magnetic features exhibited by AFC, whose presentation and analysis constitutes the rest of this work.

Figure 4 shows the FC and ZFC curves measured at 500 and 50 Oe (inset). Notice the effect of the magnetic field on the irreversibility starting temperature. The strong irreversibility between the FC and ZFC curves, its field dependence and the presence of a clear maximum at $T_{max} \approx 29$ K, which is smoothed by the application of higher fields, are usually found in spin glasses. However, these features alone are still ambiguous for they could also be explained in terms of the superparamagnetism theory, where the relatively high sharpness of the maxima would indicate an accordingly narrow volume size distribution of the magnetic clusters.

ac measurements were then performed in an attempt to clarify this issue. The dynamical behavior expected for a *good* spin glass includes the following characteristics:[20] (i) the presence of a ''cusplike'' maximum in the temperature dependence of the real part of the susceptibility (χ'), which depends very weakly on the frequency of the ac field. The data in Fig. 5 yield $p \approx 0.01$, which is nearly the same as those of the canonical spin glasses with highest p values (AuFe, PdMn). (ii) The absorption component of the ac susceptibility (χ'') exhibits a sudden onset near T_{max}. This is what actually occurs in our sample (inset of Fig. 5), where T_{max} nicely corresponds to the maximum slope points. (iii) The peak is highly affected by the application of relatively low dc fields: it smears out and shifts downwards. Figure 6 illustrates this point for AFC. The field dependence of T_{max} follows very closely the De Almeida-Thouless[21] (AT) law ($\sim H^{2/3}$). It is remarkable that this law is encountered in the dynamic behavior rather than in the static one, which is the usual case. In any manner, the AT line has been proved in several occasions, both theoretically[22] and empirically,[7] not to be solely the result of the mean-field model of phase transition, but also a possible consequence of superparamagnetic relaxation.

The observation of this set of phenomena has been often taken in the literature as sufficient to assert the presence of a spin-glass phase. However, all the commented dynamical features can be still explained in terms of phenomenological models[23] derived from the Néel theory of superparamagnetism.[24] Particular emphasis has been put on the frequency sensitivity of T_{max} as a possible distinguishing criterion;[20] nevertheless, it does not allow a clear distinction in systems with intermediate frequency dependence. Even the relative low p value of our sample (compared to typical superparamagnets) can be accounted for within the super-

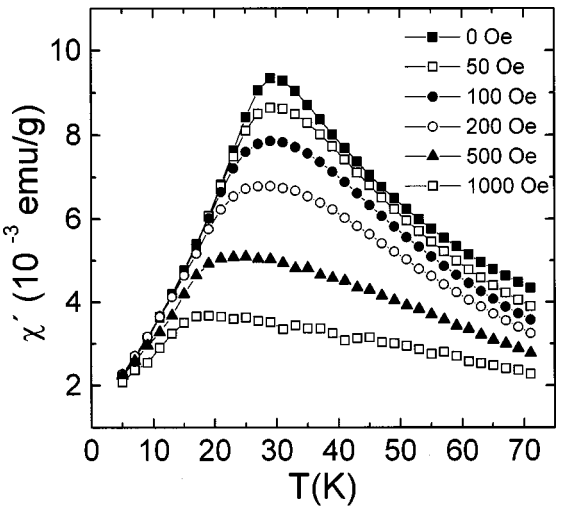

FIG. 6. Real component of the ac susceptibility vs temperature for different dc applied fields.

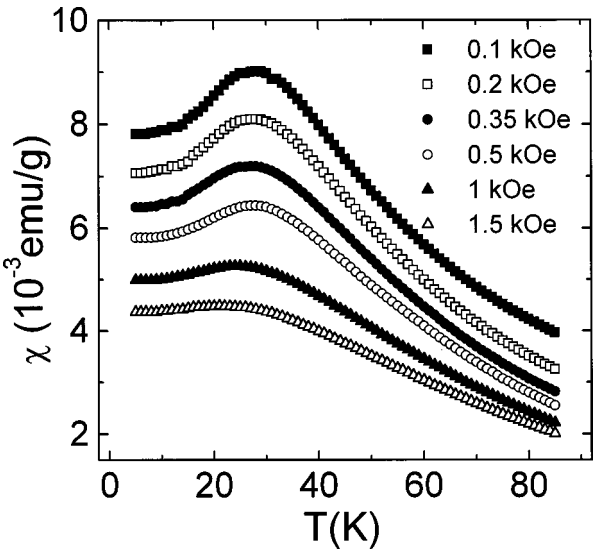

FIG. 7. FC data employed for the determination of the nonlinear coefficients.

paramagnetic framework by allowing a certain degree of interaction between the clusters.[25] The necessity of introducing such weak interparticle interactions is evidenced by the inability of the Arrhenius law $[\omega/\omega_0=\exp(-E_a/k_BT)]$ to describe the $T_{\max}$ frequency dependence (it yields unphysical values for the parameters: $\omega_0\sim10^{55}$ Hz and $E_a/k_B\sim4300$ K. In contrast, the data could be fitted with reasonable values to a Vogel-Fulcher law, $\omega/\omega_0=\exp[E_a/k_B(T-T_0)]$, where T_0 accounts for a static interaction field due to the moments of the surrounding particles, but this does not bring in any significant information since the fit is possible for several different sets of the three parameters.

Therefore, apart from experiments sensitive to *local* interactions such as muon-spin depolarization and neutron diffraction, a spin-glass phase transition cannot be definitively stated without studying the order parameter, which can be obtained from the nonlinear magnetization susceptibility $(\chi_{\rm nl})$.[16,26] In order to ascertain the occurrence of a real thermodynamic transition in AFC, we analyzed the temperature dependence of $\chi_{\rm nl}$ according to the Sherrington-Kirkpatrick mean-field model.[15] The magnetization is developed in terms of χ_0H instead of H so as to avoid an overestimation of the temperature dependence of the nonlinear terms due to a possible non-Curie-Weiss behavior of χ_0. Deviations from the Curie-Weiss law were actually observed starting from temperatures far above $T_{\max}$ ($T\approx1.5\,T_{\max}$). Thus

$$M\approx m_0+\chi_0H-b_3(\chi_0H)^3+b_5(\chi_0H)^5. \qquad (1)$$

The inclusion of the constant term accounts for possible remanent magnetization in the SQUID superconducting magnet and/or the sample. The least-squares fit of the isothermal magnetization curves built from the field-cooled data (Fig. 7) to the above expression yields the temperature dependence of χ_0, b_3, and b_5. The fit of the reciprocal linear susceptibility χ_0^{-1} versus temperature in its linear region ($T>50$ K) allowed an estimation of the interparticle interaction strength, $E_i/k_B\approx30$ K. Figure 8 shows the results obtained for the b_3 coefficient (with 20% accuracy). The relatively broad error band in the b_5 coefficient values made it less suitable for analysis. The b_3 coefficient is practically invariant in the region of interest. The spin-glass transition is characterized by a power-law critical divergence of this coefficient (in practice, an increase of at least two orders of magnitude), therefore its existence in AFC can be definitively ruled out. The application of a linear fit method resulted in the same invariance for b_3. In this method, which assumes $m_0=0$, χ_0 is obtained from the intercept to the ordinate axis in M/H versus H^2 plots for different temperatures, and then b_3 was calculated from the slope of $(1-M/\chi_0H)$ versus $(\chi_0H)^2$ plots. The lack of linearity in all this curves beyond low-field values was also symptomatic. Figure 8 shows as well the whole first nonlinear coefficient $(b_3\chi_0^3)$ in order to clarify and justify the above arguments on the power series development of the magnetization. Notice how the clear maximum in this curve vanishes after normalizing by the linear susceptibility, indicating that even the slight temperature dependence of $b_3\chi_0^3$ was due to χ_0. From this result, it is obvious that any scaling effort would have been useless. Actually, the critical isotherm did not show a linear aspect. Nor was successful the attempt of ac scaling with the data commented above. In this respect, the best fit to the law of critical slowing down in spin glasses, $\tau(\omega)=\tau_0(T/T_c-1)^{-z\nu}$, yielded unphysical values $(z\nu\approx80,\ T_c\approx2$ K).

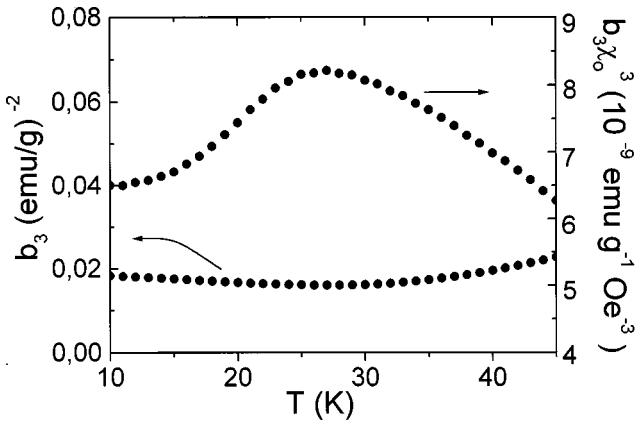

FIG. 8. Normalized (b_3) and complete $(b_3\chi_6^3)$ first nonlinear susceptibility coefficients as a function of the temperature.

Fiorani, Tholence, and Dormann also found an invariant b_3 in Fe grains dispersed in an amorphous alumina matrix by rf cosputtering and concluded that its SGL behavior (yet with a rather large p value) was to be framed in the superparamagnetism context.[7] In a different system, a mechanically alloyed FeRh nanostructured material with no separation among the crystalline grains other than their own boundaries, Hernando *et al.* detected no temperature variation of $\chi_{\rm nl}$ $(=\chi_0-M/H)$ together with a low-frequency sensitivity of $T_{\max}$, which compelled them to discard both spin glass and superparamagnetism. They ascribed the observed SGL behavior to boundary spin disorder effects after the observation of clearly shifted hysteresis loops, which became centered above the critical temperature.[6] In order to explore this possibility, we measured the hysteresis loop of AFC at 5 K after 30 KOe field cooling. No shift at all was observed in the hysteresis (Fig. 9), therefore this third source of SGL behavior seems improbable. Should it exist, it would be expected to contribute in a minor way due to the small surface to bulk ratio.

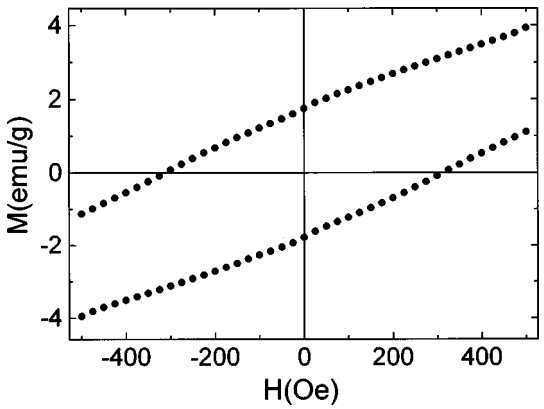

FIG. 9. Magnetization vs applied field at 5 K after zero-field cooling Notice the absence of any shift of the hysteresis loop.

On the other hand, the SGL behavior found in mechanically alloyed nanocrystalline materials has been attributed in most cases to real spin-glass transitions. That might be the case indeed and it can be theoretically justified on the basis of chemical disorder, however, further confirmation via phase transition analysis is needed. In our sample this analysis has led precisely to the exclusion of any transition. Instead, we have suggested the blocking of interacting macromoments as the origin of the observed phenomena, for it can account for the observed magnetic properties and seems feasible from a structural point of view. The Curie temperature of the nanocrystals is higher than 700 K (when structural changes start to take place) and the nature of the interaction is thought to be mainly dipolar. RKKY long-range exchange interaction through the amorphous metallic matrix cannot be ruled out, but its contribution must be secondary since the RKKY range remarkably dampens in highly disordered media (as it occurs in amorphous spin glasses[20]).

The results presented for AFC allow a final observation. Since the blocking of an assembly of interacting particles remains the most likely explanation for the observed magnetic phenomena, we must concede that the particles are essentially exchange decoupled, which, in turn, leads to conclude that the amorphous matrix is much less magnetic than the crystalline grains. Although the nanocrystals have an extra 3% Fe, such conclusion can be mainly held in terms of the differences in structure. Similar results, concerning the magnetic differences between ordered and amorphous alloys, have been found in a variety of systems.[27]

IV. CONCLUSIONS

In summary, a sample of mechanically alloyed Fe-Al-Cu, whose structure was observed by HRTEM to consist of crystalline nanoparticles embedded in an amorphous matrix of roughly the same composition, showed a magnetic behavior resembling very closely that of canonical spin glasses both in its static and dynamical manifestations. Such behavior was proved not to stem from a thermodynamic phase transition by analyzing the temperature dependence of χ_{nl}, which showed a nearly constant behavior around $T_{\max}\approx 29\,\mathrm{K}$ and not a sharp increase that could be taken for a divergence. Boundary spin disorder has been reasoned to be an improbable explanation since a well centered hysteresis loop was observed at 5 K (far below $T_{\max}$). As a result, we conclude that the fundamental source for the observed SGL phenomena is the blocking of the interacting (mainly dipole-dipole) Fe-Al-Cu solid solution nanocrystals.

ACKNOWLEDGMENT

This work was financially supported by the Spanish CYCIT under Grant No. MAT97-0294.

*FAX: 34-26-295318. Electronic address: malopez@fiap-cr.uclm.es

[1] G. F. Zhou and H. Bakker, Phys. Rev. Lett. **72**, 2290 (1994).
[2] G. F. Zhou and H. Bakker, Phys. Rev. Lett. **73**, 344 (1994).
[3] D. X. Li, K. Sumiyama, K. Suzuki, and T. Suzuki, Phys. Rev. B **55**, 6467 (1997).
[4] J. Tang, W. Zhao, C. J. O'Connor, C. Tao, M. Zhao, and L. Wang, Phys. Rev. B **52**, 12 829 (1995).
[5] L. Klein, Phys. Rev. Lett. **74**, 618 (1995).
[6] A. Hernando, E. Navarro, M. Multigner, A. R. Yavari, D. Fiorani, M. Rosenberg, G. Filati, and R. Caciuffo, Phys. Rev. B **58**, 5193 (1998).
[7] D. Fiorani, J. Tholence, and J. L. Dormann, J. Phys. C **19**, 5495 (1986).
[8] R. W. Chantrell and E. P. Wolfarth, J. Magn. Magn. Mater. **40**, 1 (1983).
[9] J. L. Tholence, Solid State Commun. **35**, 113 (1980).
[10] J. L. Tholence, Physica B **126**, 157 (1984).
[11] D. Fiorani, in *Studies of Magnetic Properties of Fine Particles and their Relevance to Materials Science*, edited by J. L. Dormann and D. Fiorani (Elsevier Science, New York, 1992), p. 135.
[12] R. H. Kodama, Salah A. Makhlouf, and A. E. Berkowitz, Phys. Rev. Lett. **79**, 1393 (1997).
[13] B. Martínez, X. Obradors, L. L. Balcells, A. Rouanet, and C. Monty, Phys. Rev. Lett. **80**, 181 (1998).
[14] B. Dieny, V. S. Speriosu, S. S. P. Parkin, B. A. Gurney, D. R. Wilhoit, and D. Mauri, Phys. Rev. B **43**, 1297 (1991).
[15] S. Kirkpatrick and D. Sherrington, Phys. Rev. Lett. **35**, 1792 (1975); Phys. Rev. B **17**, 4384 (1978).
[16] J. Chalupa, Solid State Commun. **22**, 315 (1977); **24**, 429 (1977).
[17] J. A. De Toro, M. A. López de la Torre, R. Sáez Puche, and J. M. Riveiro, J. Magn. Magn. Mater. **196-197**, 243 (1999).
[18] N. C. Halder and C. N. J. Wagner, Acta Crystallogr. **20**, 312 (1966).
[19] P. Scherrer, Nachr. Ges. Wiss. Goettingen, Math.-Phys. Kl. **26**, 98 (1918).
[20] J. A. Mydosh, *Spin Glasses: An Experimental Introduction* (Taylor & Francis, London, 1993).
[21] J. R. de Almeida and D. J. Thouless, J. Phys. A **11**, 983 (1978).
[22] L. E. Wenger and J. A. Mydosh, Phys. Rev. B **29**, 4156 (1984).
[23] J. J. Prejean and J. Souletie, J. Phys. (Paris) **41**, 1335 (1980).
[24] L. Néel, Ann. Geophys. (C.N.R.S.) **5**, 99 (1949); C. R. Hebd. Seances Acad. Sci. **252**, 4075 (1961).
[25] S. Shtrikman and E. P. Wolfarth, Phys. Lett. **85A**, 467 (1981).
[26] M. Suzuki, Prog. Theor. Phys. **58**, 1151 (1977).
[27] T. Kaneyoshi, *Introduction to Amorphous Magnets* (World Scientific, Singapore, 1992).